*FEMS Microbiology Ecology*, 2024, **100**, fiae099
DOI: 10.1093/femsec/fiae099
**Advance access publication date: 13 July 2024**
**Research Article**

# Dissolved organic phosphorus bond-class utilization by *Synechococcus*

Emily M. Waggoner [1], Kahina Djaoudi [1], Julia M. Diaz [2], Solange Duhamel [1,*]

[1]Department of Molecular and Cellular Biology, University of Arizona, 1007 East Lowell Street, Tucson, Arizona, AZ 85721, United States
[2]Geosciences Research Division, Scripps Institution of Oceanography, University of California, San Diego, La Jolla, CA 92093, United States
*Corresponding author. Department of Molecular and Cellular Biology, University of Arizona, 1007 East Lowell Street, Tucson, Arizona, AZ 85721, United States. E-mail: duhamel@arizona.edu
**Editor:** [Martin W. Hahn]

## Abstract

Dissolved organic phosphorus (DOP) contains compounds with phosphoester, phosphoanhydride, and phosphorus–carbon bonds. While DOP holds significant nutritional value for marine microorganisms, the bioavailability of each bond-class to the widespread cyanobacterium *Synechococcus* remains largely unknown. This study evaluates bond-class specific DOP utilization by *Synechococcus* strains from open and coastal oceans. Both strains exhibited comparable growth rates when provided phosphate, a phosphoanhydride [3-polyphosphate and 45-polyphosphate], or a DOP compound with both phosphoanhydride and phosphoester bonds (adenosine 5′-triphosphate). Growth rates on phosphoesters [glucose-6-phosphate, adenosine 5′-monophosphate, bis(4-methylumbelliferyl) phosphate] were variable, and neither strain grew on selected phosphorus–carbon compounds. Both strains hydrolyzed 3-polyphosphate, then adenosine 5′-triphosphate, and lastly adenosine 5′-monophosphate, exhibiting preferential enzymatic hydrolysis of phosphoanhydride bonds. The strains' exoproteomes contained phosphorus hydrolases, which combined with enhanced cell-free hydrolysis of 3-polyphosphate and adenosine 5′-triphosphate under phosphate deficiency, suggests active mineralization of phosphoanhydride bonds by these exoproteins. *Synechococcus* alkaline phosphatases presented broad substrate specificities, including activity toward the phosphoanhydride 3-polyphosphate, with varying affinities between strains. Collectively, these findings underscore the potentially significant role of compounds with phosphoanhydride bonds in *Synechococcus* phosphorus nutrition and highlight varied growth and enzymatic responses to molecular diversity within DOP bond-classes, thereby expanding our understanding of microbially mediated DOP cycling in marine ecosystems.

**Keywords:** alkaline phosphatase; dissolved organic phosphorus; phosphoanhydride; phosphoester; phosphonate; *Synechococcus*

## Introduction

The picocyanobacterium *Synechococcus* is an abundant photosynthesizer, inhabiting multiple climate zones, as well as open ocean and coastal regions (Palenik et al. 2006, Zwirglmaier et al. 2008, Tai and Palenik 2009, Sohm et al. 2016, Bock et al. 2018, Nagarkar et al. 2021). Phosphorus (P) availability is a dominant factor influencing *Synechococcus* ecophysiology and abundance, as phosphate (Pi) can be present at biologically low, colimiting, and limiting concentrations in surface mixed-layer oligotrophic regions (Krom et al. 2010, Lomas et al. 2010, Kretz et al. 2015, Djaoudi et al. 2018, Sosa et al. 2019, Yuan et al. 2024). As one strategy to cope with Pi scarcity, marine microorganisms, including *Synechococcus*, use dissolved organic phosphorus (DOP), which typically constitutes the dominant fraction of the dissolved P pool in open ocean surface waters (Lomas et al. 2010, Duhamel et al. 2014, 2021, Karl and Björkman 2015, Ranjit et al. 2024). Even in Pi-replete regions, the labile fraction of DOP is rapidly recycled (Benitez-Nelson and Buesseler 1999, Nausch et al. 2018), emphasizing the role of DOP in microbial P nutrition and its potentially significant role in sustaining primary productivity (Björkman et al. 2018, Whitney and Lomas 2019, Duhamel et al. 2021, Letscher et al. 2022).

Natural marine DOP can be classified into three P bond-classes: phosphoesters (P-esters), polyphosphates (PolyP), and phosphonates (Phn) (Kolowith et al. 2001, Young and Ingall 2010). P-esters (+V oxidation state), typically in the form of monoesters (P–O–C) and diesters (C–O–P–O–C), are the most abundant (~80%–85% of the high molecular weight dissolved organic matter) (Young and Ingall 2010). P-ester bioavailability has historically focused on monoesters (Moore et al. 2005, Wang et al. 2016, Filella et al. 2022), though there is increasing support that certain marine species can utilize diesters (Yamaguchi et al. 2005, Hull and Ruttenberg 2022). PolyP is a polymer composed of orthophosphate repeating units linked by phosphoanhydride (P–O–P) bonds and is estimated to account for ~8%–13% of the high molecular weight dissolved organic matter (Young and Ingall 2010, Diaz et al. 2016, Saad et al. 2016). While PolyP can be found in organic and inorganic forms, it is typically measured in the organic P pools as it requires prior hydrolysis to yield soluble reactive P (Armstrong et al. 1966, Karl and Tien 1992, Karl and Björkman 2015). Although poorly characterized, PolyP quantifications revealed similar relative concentrations in the North Pacific Subtropical Gyre (Diaz et al. 2008, 2016) and Indian Ocean (Martin et al. 2018) surface waters. Phosphonates (P–C) include P in its +III oxidation state and account for ~5%–10% of the high molecular weight dissolved organic matter (Young and Ingall 2010). Naturally and artificially occurring phosphonates have the potential to be bioavailable P sources for certain marine bacteria (Repeta et al. 2016, Sosa et al. 2019), marine cyanobacteria (Ilikchyan et al. 2009, 2010), and marine eukaryotic

**Received** 13 March 2024; **revised** 14 May 2024; **accepted** 12 July 2024

taxa (Wang et al. 2016, Whitney and Lomas 2019). Despite the importance of DOP, the relative bioavailability of specific bond-class compounds is poorly resolved (Karl and Björkman 2015, Diaz et al. 2016, Granzow et al. 2021).

To acquire Pi from DOP, marine microorganisms can use P-hydrolases, including alkaline phosphatases (AP), which are regulated by the Pho Regulon, itself controlled by Pi availability (Cembella et al. 1984, Duhamel et al. 2010, 2014, Santos-Beneit 2015, Huang et al. 2018, Li et al. 2019, Sisma-Ventura and Rahav 2019). APs include isoforms (phoA, phoD, and phoX) that are widely distributed in prokaryotes, including *Synechococcus* (Tetu et al. 2009, Cox and Saito 2013), and are known for hydrolyzing P-monoesters, and possibly P-diesters (Huang et al. 2018, Srivastava et al. 2021). The enzymes responsible for PolyP degradation are not well-characterized, though there is increasing evidence that marine APs may be able to hydrolyze PolyP (Martin et al. 2018, Lin et al. 2019, Adams et al. 2022). Certain coastal *Synechococcus* strains, namely CC9311 and CC9902, lack the Pho Regulon. This absence has been hypothesized to be an adaptation to their growth in P-replete environments (Su et al. 2007). The lack of this regulatory complex contrasts with its identification in both open ocean WH8102 and coastal WH5701 *Synechococcus* strains (Su et al. 2007, Scanlan et al. 2009, Tetu et al. 2009, Christie-Oleza et al. 2015, Santos-Beneit 2015). The Pho Regulon also controls the expression of the *phn* operon, a multigene complex that allows for the transport and use of phosphonates (Kamat and Raushel 2013, Tiwari et al. 2015, Stosiek et al. 2020). The *phn* operon encodes a range of P-C cleaving enzymes, including the P–C lyase complex, which supports the hydrolysis of a range of phosphonates. Additional enzymes, such as phosphonohydrolases, act on phosphonates independently of Pi availability and are present in a range of prokaryotes (McGrath et al. 1997, Benitez-Nelson et al. 2004, Quinn et al. 2007, Villarreal-Chiu et al. 2012).

Though P-esters are thought to dominate microbial DOP nutrition, recent studies using culture isolates indicate that to some microbial groups, PolyP plays an important role (Lin et al. 2016, Diaz et al. 2018, 2019, Duhamel et al. 2021, Adams et al. 2022). Specifically, picocyanobacteria strains *Prochlorococcus* MED4, MIT9312, and MIT9313, and *Synechococcus* WH8102 can grow on short-chain 3-polyphosphate (3-PolyP) as a sole source of P (Moore et al. 2005). For marine bacteria cultures of *Ruegeria pomeroyi* DSS-3, PolyP and P-ester substrates can support equivalent growth (Adams et al. 2022), while diatom cultures of the genus *Thalassiosira* exhibit preferential degradation of PolyP over P-esters (Lin et al. 2016, Diaz et al. 2018, 2019). Considering the widespread presence of *Synechococcus* and its importance in biogeochemical cycling, we assessed bond-specific bioavailability and utilization of DOP compounds to open ocean (WH8102) and coastal (WH5701) *Synechococcus* strains. We hypothesized that *Synechococcus* can hydrolyze both P-anhydrides and P-esters, possibly using AP, supporting a flexible P metabolism favoring their wide distribution across global surface waters.

# Materials and methods

## Synechococcus growth, axenicity, and cell counts

Axenic *Synechococcus* WH8102 (open ocean strain) and WH5701 (coastal strain) were obtained from the National Center for Marine Algae and Microbiota (NCMA, Bigelow Laboratories, East Boothbay, Maine). Both strains were grown in batch culture using SN media (Waterbury et al. 1986) made with aged, filtered (0.2 µm), and autoclaved (120°C, 30 min) seawater from station ALOHA (A Long-term Oligotrophic Habitat Assessment). At the late-exponential phase, cultures were transferred in triplicate to one of two SN media: (1) +Pi (45 µmol $l^{-1}$ $KH_2PO_4$; following Waterbury et al. 1986) and (2) −Pi (no $KH_2PO_4$ added; Pi below detection limit). All cultures were incubated at 25°C on a 12 h:12 h light cycle at 130 µmol $m^{-1}$ $s^{-1}$ in sterile culture flasks with a vent cap (0.22 µm hydrophobic membrane). *In vivo* fluorescence (IVF) was measured (AquaFluor®, Turner Designs) as a proxy for *Synechococcus* biomass. An aliquot of all culture treatments was inoculated in Luria-Bertani (LB, Miller) broth once per growth phase and incubated in the dark at 25°C for 3 days to verify that the cultures remained axenic during each experiment. A culture was considered axenic if the absorbance, measured at 610 nm, did not increase significantly over this time, which was the case for all samples. Over the growth curve, *Synechococcus* culture aliquots were collected, fixed (final concentration of 0.2% paraformaldehyde), and stored at −80°C until cell abundance analysis using the Guava® EasyCyte flow cytometer (Millipore). Briefly, *Synechococcus* was enumerated in unstained samples based on red fluorescence (i.e. chlorophyll) and forward scatter signals using a low flow rate of 0.24 µl $s^{-1}$ for 1 min. Instrument-specific beads (Guava® Check Kit, Luminex) were used to calibrate the instrument.

## Growth on DOP substrates

The capacity of *Synechococcus* WH8102 and WH5701 to grow on different DOP bond-classes as a sole P source was tested in −Pi SN media amended with a single DOP substrate (45 µmol $l^{-1}$ P, final concentration; Waterbury et al. 1986). To examine *Synechococcus* growth across DOP bond-classes, two P-monoesters, one P-diester, two P-anhydrides, and four phosphonates were selected as representatives of the DOP pool. Additionally, a P-monoester containing P-anhydride bonds was selected to examine growth on a DOP compound containing multiple bond-classes. Specifically, representative DOP compounds included the P-monoesters glucose-6-phosphate (Glc-6-P) and adenosine 5′-monophosphate (AMP); the P-diester bis(4-methylumbelliferyl) phosphate (BisMUF-P); the short and long chain polyphosphates: 3-PolyP and 45-polyphosphate (45-PolyP); the P-monoester and P-anhydride containing adenosine 5′-triphosphate (ATP); and the phosphonates: 4-nitrophenyl phenylphosphonate (4-NpPn), 2-aminomethylphosphonic acid (2-AEPn), methylphosphonic acid (MPn), and ethylphosphonic acid (EPn). Two separate experiments were carried out in triplicate to test growth on (1) P-monoester and PolyP substrates, and (2) a P-diester and phosphonates. Two control treatments (culture grown in +Pi and −Pi media) were carried out in triplicate for each experiment. IVF was measured daily in each treatment over ∼20 days, and cell axenicity was tested every ∼5 days. Growth rates were calculated as the slope of the best-fit line over the natural log-linear portion of the IVF curve (typically within days 0–7, except for AMP which was within days 7–13 to account for the delayed growth; Table S1).

To address the possibility of abiotic degradation of the amended DOP substrates under culture conditions, a separate experiment was conducted, measuring autohydrolysis of each DOP substrate over 20 days. Pi concentration was measured in −Pi SN media amended with a single DOP compound (36 µmol $l^{-1}$; final P concentration as in Diaz et al. 2018, 2019) and no addition of cells (Figure S1). Treatments were sampled immediately after DOP addition, and again every 5 days over a 20-day incubation period. Samples were frozen at −20°C, and Pi [or soluble reactive phosphorus (SRP)] was measured using a standard colorimetric protocol (Hansen and Koroleff 1999) on a multimode plate reader

**Table 1.** Comparative analysis of *Synechococcus* culture strains' ATP and 3-PolyP hydrolysis rates. For each strain and media type, maximum hydrolysis rates for 3-PolyP and ATP were selected (days 16–23 for WH8102 and days 7–17 for WH5701). The average ratio of ATP to 3-PolyP hydrolysis (ATP:3-PolyP) is expressed as a percentage (%). P-anhydride bond degradation alone results in a hydrolysis percentage of 66.7%. A higher percentage indicates P-ester bond degradation from ATP. T scores (T; reported as absolute values) are calculated by subtracting the ATP:3-PolyP percentage from 66.7 and then dividing by the standard error (SE). The degrees of freedom (df) and two-tailed *P*-values are included.

| | | | ATP:3-PolyP (%) | | | | |
|---|---|---|---|---|---|---|---|
| ***Synechococcus* sp.** | **Media type** | **Days** | **Avg** | **SE** | **T** | **df** | ***P*-value** |
| WH8102 | +Pi | 16–23 | 58.0 | 15.0 | 2.0 | 11 | < .0001 |
| | −Pi | 16–23 | 47.0 | 40.0 | 2.0 | 11 | .0067 |
| WH5701 | +Pi | 7–17 | 37.0 | 26.0 | 4.0 | 11 | .0102 |
| | −Pi | 7–17 | 58.0 | 28.0 | 1.0 | 11 | .0005 |

(SpectraMax® M2, Molecular Devices). Absorbance read at 880 nm was calibrated using a standard curve of monopotassium phosphate (0, 0.5, 1, 2, 5, 10, 20, 40, 50, and 75 µmol $l^{-1}$; $KH_2PO_4$). The average detection limit of Pi using this method, defined as three times the standard deviation of the triplicate blank measurements, was 0.125 ± 0.005 µmol $l^{-1}$. The calibration curve was prepared with 0.2 µm filtered ALOHA seawater with a Pi background concentration below the detection limit.

## DOP hydrolysis

The capacity of *Synechococcus* WH8102 and WH5701 to hydrolyze different DOP bond-classes was determined in the presence (whole cell) and absence (cell-free filtrate) of cells over the growth curve (Diaz et al. 2018, 2019). Some P-hydrolases are predicted to be ectoenzymes, and substantial cell-free P-hydrolase activity has been documented in diverse marine environments (Duhamel et al. 2010, Baltar et al. 2019). The inclusion of cell-free filtrate hydrolysis helped reveal the mechanisms (enzymes) involved in DOP degradation. Since the selected strains did not grow on phosphonates, only DOP compounds with P-ester and P-anhydride bonds were tested. Three substrates were selected to conduct this experiment. The short-chain 3-PolyP was tested as the representative polyphosphate substrate (P-anhydrides only). Because nucleotides ATP and AMP share the same P-ester core and contain different bond types, they were also selected. AMP was selected as the representative P-ester, while ATP, containing both P-anhydride and P-ester bonds, served as a representative with both bond-classes.

Whole cell and cell-free filtrate experiments were carried out separately. For both experiment types, *Synechococcus* strains were grown in triplicate +Pi and −Pi SN media. The +Pi and −Pi cultures were subsampled approximately every 3 days over ∼20 days to obtain whole cell and cell-free DOP hydrolysis results along each phase of the cellular growth curve.

To determine DOP hydrolysis rates on each subsampling day, aliquots (200 µl) of +Pi and −Pi treatments were amended with a single DOP substrate (3-PolyP, ATP, or AMP; 20 µmol $l^{-1}$ P, final concentration) in triplicate wells of a nontreated standard 96-well transparent microplate and incubated over 6-h. For whole cell subsamples, aliquots were directly taken from the culture flasks, while cell-free filtrate subsamples were prepared by aseptically filtering (0.2 µm) culture aliquots before DOP hydrolysis determination. The following controls were prepared in triplicate wells of the microplate and monitored in parallel: (1) an unamended treatment (addition of cells and no DOP substrate) to track Pi concentrations in the cultures over time, (2) a treatment amended with $KH_2PO_4$ (45 µmol $l^{-1}$ P, final concentration) to correct for the uptake/adsorption of Pi released from DOP by the cells (Diaz et al. 2019), and (3) boiled (15 min) filtrates amended with DOP to assess potential autohydrolysis during the 6-h incubation of the plate. Pi concentration was measured following the colorimetric protocol described above. The unamended treatment showed negligible (below detection limit) Pi release during the 6-h incubations for all subsamplings over the growth curve, ruling out the release of periplasmic (Kamennaya et al. 2020) and other cellular sources of Pi as a major factor. DOP hydrolysis rates were normalized to flow cytometry cell counts to account for biomass differences between strains and treatments.

To determine if the observed hydrolysis rates were sufficient to sustain cellular P demand (Diaz et al. 2019), the following equation was used:

$$H = Q \times g,$$

where $H$ is the maximum hydrolysis rate (amol cell$^{-1}$ day$^{-1}$), $Q$ is the P quota (amol cell$^{-1}$), and $g$ is the growth rate (day$^{-1}$). P quota values were taken from the range of values reported in Bertilsson et al. (2003), Heldal et al. (2003), Fu et al. (2006), and Lopez et al. (2016) for *Synechococcus* culture isolates (inclusive of WH8102, WH8103, WH8104, and WH7803; no published values are available for WH5701) grown in +Pi and −Pi conditions. Specifically, the minimum and maximum P quotas for cultures grown in +Pi (58.0 and 140.0 amol cell$^{-1}$, respectively) and for cultures grown in −Pi (16.0 amol cell$^{-1}$ and 25.0 amol cell$^{-1}$, respectively) were used. For each observed rate of hydrolysis, an expected growth rate ($g$) was calculated using the maximum hydrolysis rates (days 11–21 for WH8102, days 11–20 for WH5701) and expressed as a proportion of the observed +Pi growth rate. Ratios greater than 1 indicate that the observed DOP hydrolysis rates were sufficient to sustain P demand similar to +Pi (Table S2).

Comparative analysis was carried out between ATP and 3-PolyP to determine if the P-ester bond of ATP is likely degraded alongside the P-anhydride bond (Table 1). Four consecutive subsampling days, encompassing peak hydrolysis rates, were selected for each strain and media type in the whole cell experiment. As ATP contains a P-ester and two P-anhydride bonds, the substrate provides bond-class hydrolysis on a single substrate. Under complete hydrolysis of either ATP or 3-PolyP, three orthophosphates can be released; however, a maximum of two and three orthophosphates from ATP and 3-polyP, respectively, can be released by hydrolysis of P-anhydride bonds alone. Therefore, under complete P-anhydride degradation, where the P-ester bond of ATP remains intact, the ATP:3-PolyP hydrolysis ratio is 2:3 (or 66.7%) (Diaz et al. 2018). If the ATP:3-PolyP hydrolysis ratio is >66.7%, it suggests the likely degradation of the P-ester bond of ATP as well (Table 1).

## Cell-free proteins

For *Synechococcus* extracellular protein identification following growth in minimal P, WH8102 and WH5701 were grown in triplicate 500 ml culture flasks in −Pi SN media amended with 1 µmol $l^{-1}$ $KH_2PO_4$; a concentration previously determined as being low enough to induce P-stress while still maintaining biomass (Cox and Saito 2013). In the stationary phase, each culture triplicate was transferred to an autoclaved 250 ml polypropylene bottle and centrifuged at 3200 r $m^{-1}$ for 20 min at 4°C. The supernatant was filtered using a sterile disposable vacuum filtration system (0.2 µm). Filtrate (70 ml) was added to a prerinsed Centricon spin column (Tris Buffer; 20 mmol $l^{-1}$, pH = 8) and centrifuged at 3200 r $m^{-1}$ for 45 min at 4°C. The procedure was repeated three times for both strains and triplicates. The sample was then dialyzed twice with Tris buffer (20 mmol $l^{-1}$, pH = 8), and the concentrate was recovered and brought to a final volume of ∼500 µl using Tris Buffer. A QuickStart Bradford protein assay kit (Bio-Rad), calibrated using a standard curve of gamma globulin, was used to ensure that the samples contained enough protein (minimum of 100 µg $ml^{-1}$) for further analyses. According to the manufacturer's instructions, a trypsin digest was carried out on 10.5 µl of each triplicate using an in-solution digestion kit (ThermoScientific). Peptide samples were analyzed at the Proteomics and Mass Spectrometry facility at the University of Georgia on a Thermo-Fisher LTQ Orbitrap Elite mass spectrometer coupled with a Proxeon Easy NanoLC system (Waltham, MA, USA) following Adams et al. (2022). Peptides were mapped to the *Synechococcus* genome (NCBI BioProject PRJNA230) (Palenik et al. 2003, McCarren et al. 2005). The protein set was searched in BLASTP against NCBI nonredundant databases, and accession numbers were cross-referenced on UniProt to confirm putative function and identify APs.

## MUF-P displacement

The affinity of *Synechococcus* APs for different DOP model substrates with varying P bond-classes was examined through its ability to inhibit the hydrolysis of the fluorogenic substrate 4-methylumbelliferyl phosphate (MUF-P) (Nedoma et al. 2007). Late-exponential phase samples of −Pi cultures were incubated in triplicate wells of a black, nontreated 96-well microplate for each *Synechococcus* strain. Either a PolyP (3-PolyP, 45-PolyP), P-ester (ATP, AMP, Glc-6-P), or phosphonate (MPn) was added in a series of concentrations (0, 2, 5, 10, 20, 40, 70, and 100 µmol $l^{-1}$; final P concentration) with a single concentration of MUF-P. The selected DOP substrates exhibit no apparent chemical properties conducive to irreversible binding (Reid and Wilson 1971, Holtz et al. 1999, Whisnant and Gilman 2002). The MUF-P concentration was 10% of the previously determined Michaelis–Menten constant ($K_m$). This value was established by incubating 200 µl of each *Synechococcus* strain with a range of MUF-P concentrations (0 to 20 µmol $l^{-1}$), following the equation:

$$V = Vmax \times S/Km + S,$$

where S and V are the concentrations of MUF-P and the MUF-P hydrolysis rates, respectively.

For each tested DOP model substrate, MUF-P hydrolysis velocity was determined fluorometrically (excitation/emission: 359/449, 4-methylumbelliferone –MUF), using a multimode plate reader (SpectraMax® M2, Molecular Devices) at multiple time points over an incubation period of 24-h to ensure linearity. MUF-P hydrolysis inhibition (%) is defined as a decrease of MUF-P hydrolysis velocity over the tested range of model DOP substrate concentrations relative to the control without DOP (receiving only a single MUF-P concentration). To determine $IC_{50}$, which corresponds to the DOP concentration that causes 50% inhibition of MUF-P, data (both MUF-P hydrolysis inhibition and DOP concentrations) were fitted with a sigmoid function as described in Nedoma et al. (2007). Because the amended MUF-P concentration was 10% of the $K_m$ for both strains (i.e. 10% of 5 µmol $l^{-1}$ = 0.5 µmol $l^{-1}$), the $IC_{50}$ value can be directly expressed as the inhibition constant $K_i$ (Nedoma et al. 2007). As such, a DOP substrate with a low binding affinity will have a high $K_i$, as a higher DOP concentration is required to inhibit MUF-P hydrolysis.

## Data and statistical analyses

Statistical analyses for the displacement experiment were carried out in MATLAB. DOP concentrations that inhibit MUF-P hydrolysis velocities by 50% were compared using a one-way ANOVA. Flow cytometry data were processed using FCS Express 7. All remaining data analyses were performed in Microsoft Excel and GraphPad Prism 8. Substrates were compared following a two-way ANOVA and *post hoc* testing with Dunnet's method (between experimental and control treatments) to assess culture growth on DOP. Differences in cell-normalized hydrolysis rates were evaluated using repeated measures ANOVA and *post hoc* testing with either Tukey's honest significant difference (between the two strains and substrates under each growth condition) or Dunnett's (between experimental and control treatments) method.

# Results

## Growth on phosphoanhydrides, phosphoesters, and phosphonates

Axenic cultures of *Synechococcus* WH8102 and WH5701 grew on a variety of DOP compounds, inclusive of P-esters and P-anhydrides bond-classes, as a sole source of added P (Fig. 1, Table S1). Both strains grew on P-anhydride containing compounds 3-PolyP, 45-PolyP, and ATP with growth rates equivalent to ($P > .05$; one-way ANOVA), or greater than ($P < .05$; one-way ANOVA) the +Pi treatment (i.e. > 0.5 $day^{-1}$; Table S1). Additionally, both strains grew on the P-ester Glc-6-P similar to the +Pi treatment ($P < .01$ for WH5701, $P = .3814$ for WH8102; one-way ANOVA). However, on the P-ester AMP, both strains exhibited growth rates significantly lower than the +Pi control ($P < .0001$; one-way ANOVA). Specifically, for WH8102, growth on AMP was equivalent to growth on −Pi ($P > .05$; one-way ANOVA), and despite a slight increase in IVF for WH5701 on AMP by day 14, its growth rate only reached half that on +Pi (Fig. 1B). Neither strain grew on phosphonates MPn, EPn, 2-AEPn, and 4-NpPn, with IVF values significantly lower than the +Pi control ($P < .05$; two-way ANOVA, Fig. 1C and D) and negligible growth rates, similar to the −Pi treatment (< 0.15 $day^{-1}$; Table S1). Growth on the P-diester BisMUF-P varied between strains. For WH8102, IVF values steadily increased, albeit lower than +Pi and with a growth rate half that of +Pi (0.20 ± 0.02 $day^{-1}$; Table S1), while for WH5701, IVF values remained negligible over the growth curve and exhibited a growth rate (0.11 ± 0.01 $day^{-1}$; Table S1) 3-fold lower than +Pi, similar to −Pi. Over the 20-day autohydrolysis experiment, DOP with P-anhydride bonds (3-PolyP, 45-PolyP, and ATP) were autohydrolyzed. Low abiotic degradation occurred in the initial 5 days; by day 20, 19.0 ± 1.5 µmol $l^{-1}$ of 3-PolyP, 9.0 ± 1.0 µmol $l^{-1}$ of ATP, and 7.0 ± 6.0 µmol $l^{-1}$ of 45-PolyP were abiotically degraded (Figure S1). However, the rates of abiotic degradation were negligible compared to the whole cell DOP hydrolysis rates measured over 6-h (see below).

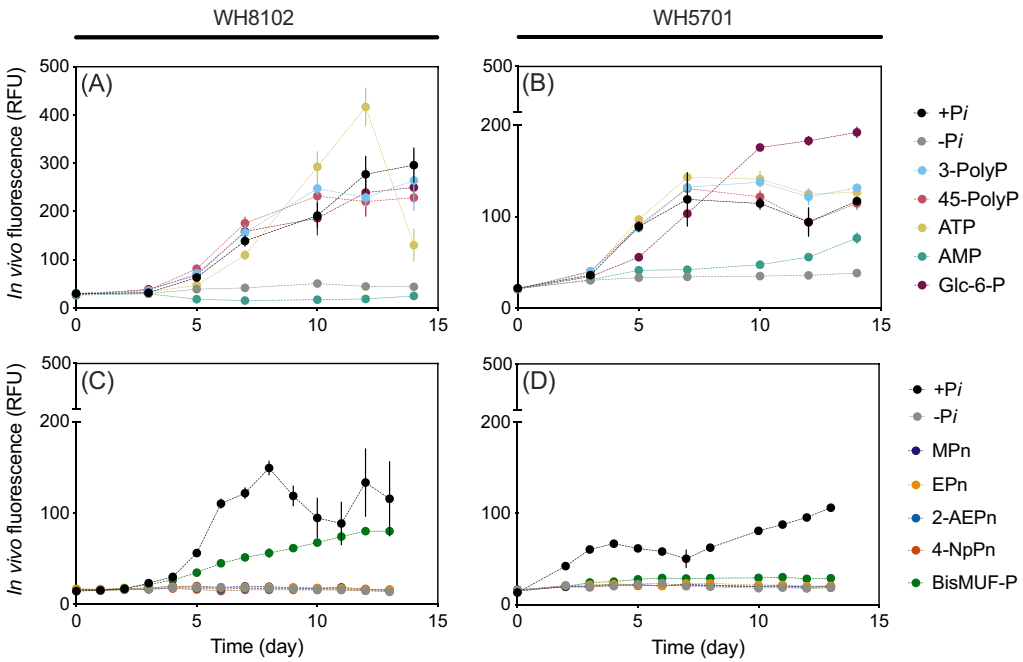


**Figure 1.** *Synechococcus* growth on DOP. *Synechococcus* WH8102 (A) and (C) and WH5701 (B) and (D) were grown on a single DOP substrate as the sole P source in two experiments, assessing IVF (RFU; y-axis) over time (day; x-axis) for P-monoesters and polyphosphates (A) and (B), as well as a P-diester and phosphonates (C) and (D). Representative DOP compounds included the P-monoesters Glc-6-P and AMP; the P-diester BisMUF-P; the short and long chain polyphosphates: 3-PolyP and 45-PolyP; the P-monoester and P-anhydride containing ATP; and the phosphonates: 4-NpPn, 2-AEPn, MPn, and EPn. Error bars indicate one standard deviation of the mean of three biological replicates. All symbols not visible at the x-axis showed negligible growth, not significantly different ($P > .05$) from the −Pi treatment.

## DOP hydrolysis

To assess P-ester and P-anhydride degradation, hydrolysis rates of a representative P-anhydride (3-PolyP) and P-ester (AMP), as well as a DOP compound with both P-anhydride and P-ester bonds (ATP), were measured for *Synechococcus* WH8102 and WH5701 grown in +Pi and −Pi SN media (Fig. 2). All tested DOP substrates showed autohydrolysis below the detection limit over the 6-h incubation for the whole cell and cell-free filtrate experiments. In the whole cell experiment, hydrolysis rates per cell generally increased with time over the growth curve, consistent with the decrease in media Pi concentration. Higher per-cell hydrolysis rates were observed in the −Pi treatment relative to +Pi ($P < .05$; one-way ANOVA; Fig. 2). Specifically, for WH8102, maximum hydrolysis rates for 3-PolyP, ATP, and AMP were ∼24-fold higher in the −Pi treatment than in the +Pi treatment. For WH5701, maximum hydrolysis rates in the −Pi treatment were 32.0 ± 14.0-fold higher for 3-PolyP, 2.5 ± 1.0-fold higher for ATP, and 3.0 ± 2.0-fold higher for AMP, in comparison to the +Pi treatment. Regardless of strain and Pi availability, throughout the experiments, 3-PolyP hydrolysis rates were significantly higher than ATP, and ATP hydrolysis rates were significantly higher than AMP ($P < .05$; Fig. 2C–F). Maximum DOP hydrolysis rates were observed for 3-PolyP in the −Pi treatment at the onset of the stationary phase, reaching 502.0 ± 17.0 amol cell$^{-1}$ h$^{-1}$ for WH8102 and 406.0 ± 8.5 amol cell$^{-1}$ h$^{-1}$ for WH5701.

In the final 2 weeks, corresponding to the highest observed DOP hydrolysis rates (Diaz et al. 2018), the ATP:3-PolyP hydrolysis ratio was less than 2:3, or 66.7%, for both strains and Pi treatments. This result suggests that the P-ester bond of ATP remained intact while the P-anhydride bond was hydrolyzed (Table 1). In the early phase of the growth curve, AMP hydrolysis rates were below detection in both strains and Pi treatments. By day 23 for WH8102 grown on +Pi, low but consistent hydrolysis rates were observed (4 ± 1 amol cell$^{-1}$ h$^{-1}$; Fig. 2C). For the remaining strains and media types, while AMP hydrolysis was observable on certain individual sampling days, rates did not increase over time ($P > .05$; two-way ANOVA; Fig. 2D–F).

DOP hydrolysis activity was verified in the cell-free filtrate (Figure S2), indicating the presence of cell-free P-hydrolase enzymes. DOP hydrolysis rates in −Pi filtrates were observed over the growth curve ($P < .001$; one-way ANOVA; Figure S2E and F), with 3-PolyP hydrolysis rates significantly higher than ATP hydrolysis rates (Figure S2E and F). AMP hydrolysis rates were negligible in all filtrates. Maximum hydrolysis rates observed in the filtrates occurred for 3-PolyP in the −Pi treatment on day 21 (471.0 ± 11.0 amol cell$^{-1}$ h$^{-1}$ for WH8102, 220.0 ± 1.0 amol cell$^{-1}$ h$^{-1}$ for WH5701; Figure S2E and F). DOP hydrolysis by WH8102 grown in +Pi media was minimal over the growth curve, with no significant difference over time and between treatments ($P = .6250$; Figure S2C). Hydrolysis rates were minimal for WH5701 grown in +Pi media, except on day 21 (64.0 ± 3.0 amol cell$^{-1}$ h$^{-1}$ for 3-PolyP, 23.0 ± 1.0 amol cell$^{-1}$ h$^{-1}$ for ATP, 1.0 ± 0.5 amol cell$^{-1}$ h$^{-1}$ for AMP; Figure S2D).

## Cell-free proteins

Overall, 43 and 25 proteins were present in the exoproteome of Pi-limited WH8102 and WH5701, respectively. Of that, 30% for WH8102 and 16% for WH5701 were hypothetical unidentified proteins (Tables S3 and S4). Among the annotated proteins were ones associated with phosphate acquisition pathways. A phosphate ABC transporter was identified in WH8102 (CAE07533.1) and WH5701 (EAQ75702.1). For WH8102, putative APs (CAE08906.1 and CAE8314.1), phosphorylase (CAE06671), and nucleoside diphosphate kinase (CAE08873.1) were present, though not across all

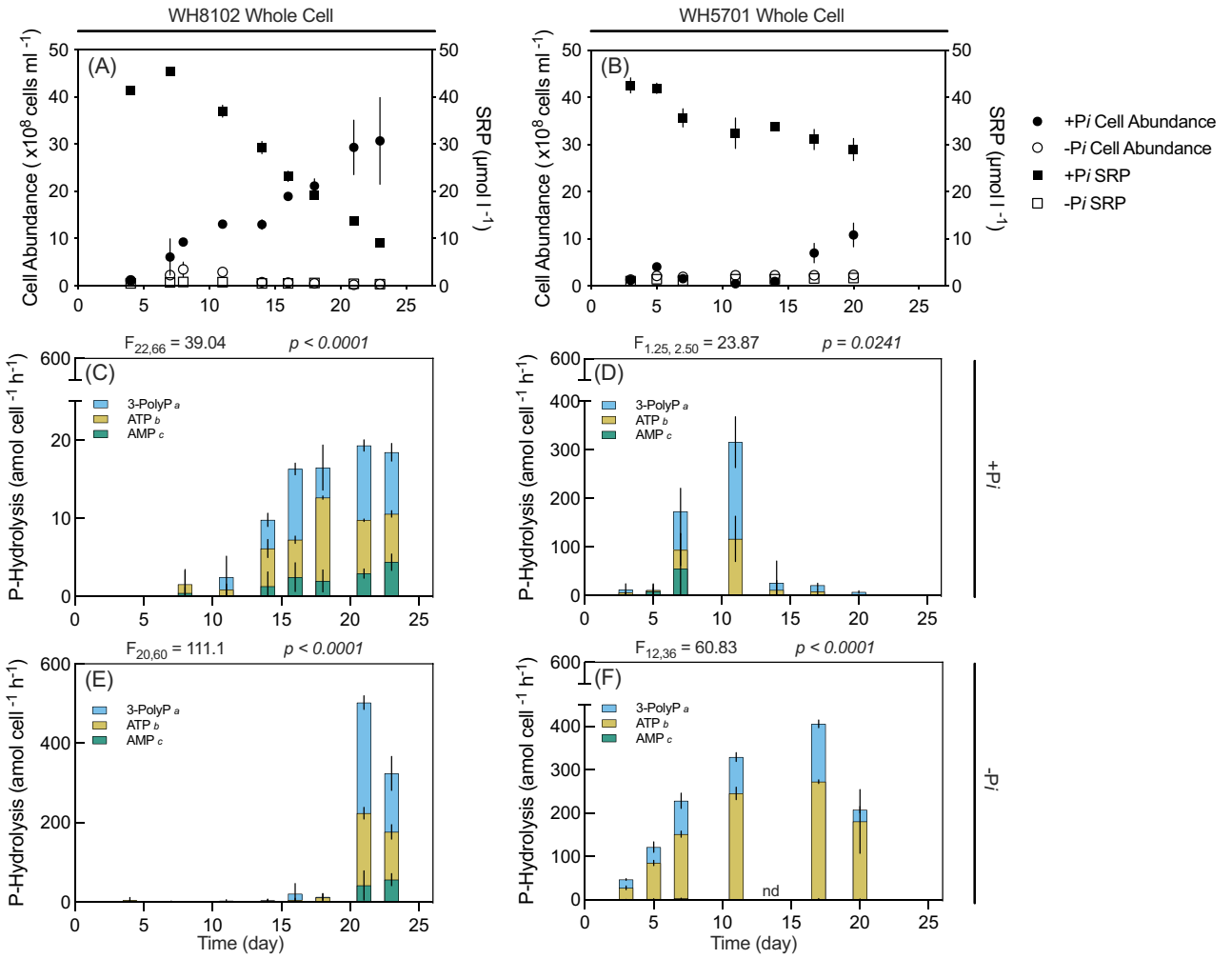


**Figure 2.** *Synechococcus* DOP hydrolysis. SRP concentrations (µmol $l^{-1}$; squares) and cell abundance (×$10^8$ cells $ml^{-1}$; circles) in Pi-replete (+Pi; filled symbols) and Pi-deplete (−Pi; empty symbols) media are displayed over time (day) for WH8102 (A) and WH5701 (B). P-hydrolysis rates on selected model DOP substrates (3-PolyP, ATP, and AMP; amol $cell^{-1}$ $h^{-1}$) in +Pi (C) and (D) and −Pi (E) and (F) are normalized to cell abundance. P-hydrolysis rates are represented as overlapping bars. Error bars indicate one standard deviation of the mean of biological triplicates. Statistical results from repeated measures ANOVA are provided above each P hydrolysis plot (C)–(F), indicating the significance of DOP hydrolysis rates throughout the experiment. Results from the pairwise *post hoc* comparison of each DOP source *via* Tukey's honest significant difference test are provided next to the legend entries. DOP sources lacking a shared letter differ significantly ($P < .05$). Days in which hydrolysis rates were not collected are denoted as "no data" (nd).

replicates (replicates 2–6, replicates 2 and 5, replicates 4–6, and replicates 2, 4–6; respectively). Among the identified porins, somSYNW2224 (CAE08739.1) was previously shown to be upregulated under Pi stress. For WH5701, a putative AP (EAQ75607.1) and protein phosphatase 2C (EAQ76317.1) were the only (alongside the ABC transporter) proteins present with a known association with phosphate acquisition pathways.

## MUF-P displacement

To test substrate specificities of *Synechococcus* APs across bond-classes, AP activity was measured using the fluorogenic substrate MUF-P with and without the addition of competing DOP substrates in Pi-deplete cultures (Fig. 3). Specifically, P-anydrides (3-PolyP and 45-PolyP), P-esters (Glc-6-P and AMP), a substrate with both P-anhydride and P-esters (ATP), and a phosponate (MPn) were tested. All DOP substrates resulted in a concentration-dependent decrease of MUF-P hydrolysis by WH8102 (Fig. 3A). At a DOP addition of 70 µmol $l^{-1}$, Glc-6-P, AMP, and ATP resulted in a reduction in MUF-P hydrolysis ranging between 58% and 71%, followed by 3-PolyP at ∼50%, and finally 45-PolyP and MPn at ∼20%. In comparison, the response of WH5701 was generally muted; by 100 µmol $l^{-1}$ DOP additions, MUF-P hydrolysis decreased by ∼45% for AMP, ∼20% for Glc-6-P, 3-PolyP, 45-PolyP, and ATP, and ∼10% for MPn (Fig. 3B). The inhibition constant, $K_i$, which corresponds to the DOP substrate concentration necessary to inhibit MUF-P hydrolysis by 50%, reflects the binding affinity (the smaller the $K_i$, the greater the binding affinity; Table 2). For WH8102, $K_i$ was lowest for Glc-6-P, AMP, and 3-PolyP (∼7–11 µmol $l^{-1}$), then ATP (∼24 µmol $l^{-1}$) and could not be calculated for long-chain 45-PolyP and MPn. For WH5701, $K_i$ values could not be calculated for short and long-chain PolyP, as well as MPn and AMP, and required high concentrations of Glc-6-P and ATP (117–125 µmol $l^{-1}$) addition to inhibit MUF-P hydrolysis by 50% (Table 2).

## Discussion

The primary objective of this study was to assess the bond-specific bioavailability and utilization of DOP compounds to *Synechococcus*. For both the open ocean strain (WH8102) and the coastal strain (WH5701), our results indicate a preference for the enzymatic hy-

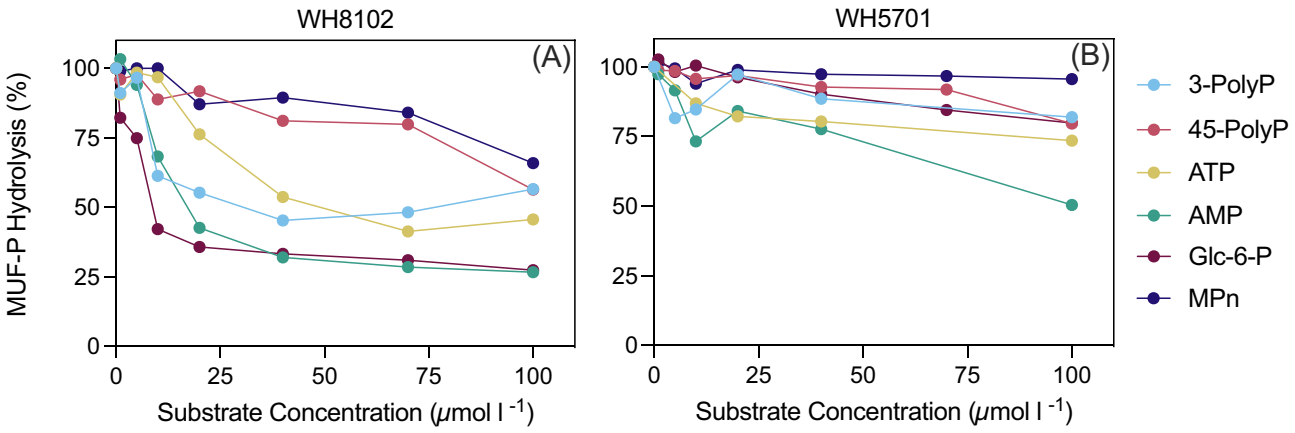


**Figure 3.** *Synechococcus* MUF-P hydrolysis inhibition by DOP. DOP substrates were applied at six different concentrations (x-axis; 0–100 μmol $l^{-1}$) in the presence of 4-methylumbelliferyl phosphate (0.5 μmol $l^{-1}$; MUF-P) for Pi-deplete *Synechococcus* WH8102 (A) and WH5701 (B). MUF-P hydrolysis, represented as a percentage (%) of the control (no DOP addition), is displayed on the *y*-axis. Dots represent the average of three biological replicates, and error bars are omitted for visual clarity. Biological triplicates typically agreed to within ± 9%.

**Table 2.** Inhibition constants for the displacement of MUF-P by DOP. Inhibition constants ($K_i$), which correspond to the concentrations necessary for half saturation of phosphatases by different DOP substrates, are presented for *Synechococcus* strains WH8102 and WH5701. DOP substrates included short and long chain polyphosphates: 3-PolyP and 45-PolyP; the P-monoester and P-anhydride containing adenosine 5′-triphosphate (ATP); the P-monoesters AMP and Glc-6-P; and phosphonate MPn. Treatments in which the DOP addition did not result in a 50% (at minimum) 4-methylumbelliferyl phosphate (MUF-P) inhibition are denoted as "not applicable" (n.a.).

| | $K_i$ constant (μmol $l^{-1}$) | | | | | |
|---|---|---|---|---|---|---|
| | **3-PolyP** | **45-PolyP** | **ATP** | **AMP** | **Glc-6-P** | **MPn** |
| **WH8102** | 13 ± 4 | n.a. | 24 ± 5 | 11 ± 3 | 7 ± 3 | n.a. |
| **WH5701** | n.a. | n.a. | 125 ± 37 | n.a. | 117 ± 12 | n.a. |

drolysis of DOP compounds containing P-anhydride bonds (i.e. 3-PolyP, 45-PolyP, and ATP).

## Growth on phosphoanhydrides, phosphoesters, and phosphonates

*Synechococcus* is a widespread cyanobacterium that is frequently exposed to low Pi concentrations, suggesting the need for a mechanism to cope with Pi scarcity (Lomas et al. 2010, Duhamel et al. 2014, 2021, Karl and Björkman 2015). DOP can serve as a P source in addition to Pi, though the DOP pool contains a range of bond types of unknown bioavailability for the microbial community (Karl and Björkman 2015, Hull and Ruttenberg 2022). Although it is widely believed that P-esters play a predominant role in microbial interactions with DOP (i.e. Karl and Björkman 2015), our results indicate that *Synechococcus* consistently exhibits growth on DOP substrates containing P-anhydrides, shows negligible growth on phosphonates, and displays substrate-dependent growth on P-esters.

PolyP only accounts for ∼8%–13% of high molecular weight dissolved organic matter (Young and Ingall 2010, Diaz et al. 2016, Saad et al. 2016), and 1%–5% of the DOP pool in coastal environments (Bell et al. 2017, 2020). That said, both the open ocean and coastal *Synechococcus* strains exhibited robust growth when cultured with P-anhydride containing compounds (specifically, 3-PolyP, 45-PolyP, and ATP), comparable to their growth with Pi as the sole P source (Fig. 1). These results indicate that the selected P-anhydride compounds are bioavailable to both strains, which builds on prior results for WH8102 (Moore et al. 2005). While phosphonate utilization pathways, such as transport genes (*phnDCE*), have been previously identified for *Synechococcus* (Moore et al. 2005, Ilikchyan et al. 2009, Shah et al. 2023), neither strain grew on phosphonates as a sole P source. Similarly, Shah et al. (2023) recently identified a lack of WH8102 growth on methylphosphonate, prompting the reinterpretation of its *phnDCE* genes as regulatory factors in Pi transport.

Phosphoesters, including diesters and monoesters, comprise most of the high molecular weight dissolved organic matter (∼80%–85%; Young and Ingall 2010), as well as coastal environment DOP pool (∼60% and ∼30%, respectively; Bell et al. 2020). Phosphodiesterase and phosphomonoesterase activity in marine environments suggest that P-diesters are less bioavailable than P-monoesters (Sato et al. 2013). Here, *Synechococcus* strains exhibited varying growth patterns when provided the P-diester BisMUF-P. WH8102 displayed an initially stunted growth curve that eventually increased, reaching maximum IVF values similar to Pi. In contrast, WH5701 demonstrated minimal growth on BisMUF-P (Fig. 1) These results imply that P-diesters may be more bioavailable to strains from the open ocean, where Pi is frequently limited or colimited, compared to coastal environments (Moore et al. 2013, Browning and Moore 2023). The delayed growth also suggests that for the open ocean strain, consistent and prolonged exposure to P-diesters may be required for the culture to employ a mechanism for utilization. This could include producing phosphodiesterases or AP that can hydrolyze P-monoesters and P-diesters (Srivastava et al. 2021).

*Synechococcus* strains displayed diverse growth responses when exposed to P-monoesters. Both strains grew on Glc-6-P similar to the +Pi treatment (Table S1); a result that aligns with *Synechococcus* WH7803 Pi cleavage of Glc-6-P (Donald et al. 1997). However, WH8102 failed to grow on AMP, and although WH5701 showed slight growth on AMP, it was delayed, and far less than the +Pi treatment (Fig. 1). This is in agreement with the low and undetectable rates of AMP hydrolysis in cultures grown in +Pi or −Pi

conditions (Fig. 2). The delayed growth on AMP implies that similar to P-diester BisMUF-P, the culture may require prolonged and consistent exposure to AMP for sustained growth. It is possible that WH5701 could utilize AMP *via* direct uptake and/or low (undetectable) rates of enzymatic hydrolysis. However, for *E. coli*, enzymatic cleavage of AMP by 5′-nucleotidase (5′-NT) is necessary for subsequent uptake of Pi (Yagil and Beacham 1975), and to our knowledge, there is no evidence for AMP direct uptake by *Synechococcus*. Although 5′-nucleotidase is present in the *Synechococcus* genome, it was not identified in either strain in the exoproteome analysis. Overall, these results suggest that different P-esters exhibit varying levels of bioavailability, emphasizing the importance of substrate diversity and complexity of P cycling in marine environments.

## DOP hydrolysis fulfilling P demand

In agreement with their growth on P-anhydride substrates as a sole P source, both −Pi strains hydrolyzed 3-PolyP and ATP. Hydrolysis rates of 3-PolyP and ATP consistently and largely exceeded P demand for growth, in both strains grown in +Pi or −Pi media, and assuming a range of P quotas (Table S2). For WH8102 in +Pi, AMP hydrolysis was sufficient in meeting the P demand only if the minimum P quota was assumed, while for WH5701 in +Pi, hydrolysis rates were insufficient regardless of the P quota. AMP hydrolysis was not detectable for WH8102 and WH5701 in −Pi until day 21 and 20, respectively, at which point, despite being substantially lower than 3-PolyP and ATP hydrolysis, met the P demand. Culture growth on DOP substrates was only monitored for 14 days, at which point cultures on +Pi and DOP, supporting equal growth, had reached the stationary phase for several days. Therefore, it is possible that longer incubations would have been necessary to observe sustained growth of both strains on AMP.

DOP hydrolysis was observed over the growth curve even in the +Pi media with background Pi concentrations at 34.0 ± 1.0 µmol $l^{-1}$ for WH5701 and 29.0 ± 1.5 µmol $l^{-1}$ for WH8102 by day 14; Fig. 2A and B). Previous studies documented DOP hydrolysis in natural communities under relatively high Pi concentrations (Benitez-Nelson and Buesseler 1999, Nausch et al. 2018). The measurable release of Pi into the media indicates a lack of strict coupling between DOP hydrolysis and Pi uptake. These combined results suggest that *Synechococcus* P-hydrolase enzymes, whether cell-free or cell-associated, liberate Pi into their environment, potentially offering a source for assimilation by other microbes. These results are consistent with the high AP activity measured across diverse natural environments with different Pi concentrations (Duhamel et al. 2011, Thomson et al. 2019). Given that growth rates on the three P-anhydride substrates either equaled or surpassed those on the +Pi control and considering that the hydrolysis of DOP containing P-anhydride bonds exceeded the estimated P growth demand, these combined results strongly support the capability of both strains to thrive on P-anhydride compounds.

## Preferential hydrolysis of the phosphoanhydride bond

Across strains and Pi availability, 3-PolyP hydrolysis rates were higher than ATP hydrolysis rates, and both were higher than AMP hydrolysis rates, confirming the preferential hydrolysis of the P-anhydride bond. Comparative analysis between ATP and 3-PolyP aims to assess whether the P-ester bond of ATP degrades alongside the P-anhydride bond (Diaz et al. 2018). For each strain and media type, the ATP:3-PolyP hydrolysis ratio consistently remained below 2:3. This observation suggests that the P-anhydride bond of ATP was degraded while the P-monoester bond of ATP remained intact. Similar results have been reported in the case of the open ocean diatom *Thalassiosira* sp. CCMP1005 and CCMP1014, as well as coastal *Thalassiosira* sp. CCMP 1335 (Diaz et al. 2018). These consistent patterns underscore the potential significance of the P-anhydride bond specificity in microbial DOP bioavailability.

## Cell-free filtrate P-Hydrolases

Marine plankton can obtain P from the hydrolysis of DOP using their cell-surface-associated enzymes (Cembella et al. 1984, Ammerman and Azam 1985). Some of these enzymes can also be liberated from the cell by secretion or upon death (cell lysis or sloppy feeding), which contributes to the cell-free P-hydrolase activity measured across Pi-replete and Pi-deplete marine environments (Duhamel et al. 2010, Baltar et al. 2019). Using cell-free culture filtrates from both strains of *Synechococcus*, we found negligible hydrolysis of the three tested DOP substrates under +Pi treatment but high hydrolysis rates of 3-PolyP and ATP in the −Pi cultures (Figure S2), confirming the presence of enzymes that act on DOP. While the cell-free filtrate is expected to include a mixture of naturally and artificially released extracellular enzymes (i.e. via filtration), this method allows us to narrow down the enzymes potentially involved in DOP hydrolysis.

Both *Synechococcus* strains hydrolyzed PolyP in the whole cell and cell-free experiments, suggesting the presence of an enzyme that can specifically hydrolyze P-anhydrides. The exoproteome of Pi-depleted strains revealed AP isoforms phoX and phoA (for WH8102) and unidentified AP (for WH5701; accession EAQ75607.1). The previously reported genome of both strains contain enzymes known for acting on PolyP and P-esters, including AP isoforms phoA and phoX; and 5′-nucleotidase (5′-NT) and polyphosphatase (ppX) (Moore et al. 2005, Scanlan et al. 2009, Tetu et al. 2009, Kutovaya et al. 2013, Christie-Oleza et al. 2015). Our results did not have PolyP-specific enzymes, so the observed extracellular PolyP hydrolysis is likely not dominated by PolyP-specific enzymes. This result aligns with the outcome of Adams et al. (2022). It does not exclude the possibility of direct low molecular weight PolyP uptake followed by interactions with ppK (synthesis and degradation) (Parnell et al. 2018) and ppX (degradation) or the potential for a low biomass sample (resulting from growth on minimal Pi) to impact the detection of additional enzymes in our samples.

## AP flexibility

Following the presence of APs in both *Synechococcus* strains, matched with 3-PolyP and ATP hydrolysis and the absence of PolyP specific enzymes, it is likely that APs play a role in the hydrolysis of P-esters and PolyP in *Synechococcus*. Though it is generally assumed that APs only hydrolyze P-monoesters (Tiwari et al. 2015), there is increasing evidence of AP substrate flexibility. APs from *E. coli* and calf intestine can cleave P-anhydride bonds (Yoza et al. 1997, Huang et al. 2018). Long-chain PolyP substrates, up to 800 monomers, may be cleaved by mammalian AP depending on the concentration and ambient pH levels, indicating that AP substrate specificity may vary (Lorenz and Schröder 2001). To test this, we determined the ability of P-ester, P-anhydride, and phosphonate substrates to compete with MUF-P for the reaction of APs from *Synechoccocus* (Fig. 3, Table 2).

The MUF-P displacement experiments provide insight into the relative affinity of AP for the DOP bond-classes. All tested substrates inhibited MUF-P hydrolysis by WH8102, indicating that *Synechococcus* WH8102 APs have broad substrate specificities (Fig. 3, Table 2), similar to results reported from the bacterial copiotroph *R. pomeroyi* (Adams et al. 2022). Specifically, P-esters Glc-

6-P and AMP exhibited the highest MUF-P inhibition, followed by ATP and short-chain 3-PolyP. Long-chain 45-PolyP and MPn also resulted in a decrease in MUF-P hydrolysis. However, 100 µmol $l^{-1}$ of each substrate was required to reach the result of other P-anhydrides at 30 µmol $l^{-1}$, suggesting a low AP-binding affinity for both long-chain polyphosphate and phosphonate MPn. These results suggest a short-chain PolyP preference by *Synechococcus* WH8102 APs. This contradicts the results of *R. pomeroyi* (Adams et al. 2022), possibly indicating different AP flexibilities across microbial groups.

For WH5701, the response to DOP was muted, suggesting a lower AP affinity for the selected DOP substrates in the tested concentration range. At high DOP concentrations (100 µmol $l^{-1}$), P-ester and PolyP substrates decreased MUF-P hydrolysis, though less than 50%, while phosphonate MPn did not. Since we measured high hydrolysis rates of ATP and 3-polyP via Pi production assays, the overall low AP affinity for these substrates suggests that WH5701 likely produces enzymes that can hydrolyze PolyP and P-esters better than synthetic MUF-P. This result also highlights the importance of studying multiple strains within *Synechococcus* when considering enzymatic responses.

## Conclusion

There is growing evidence that phosphoanhydrides, in particular PolyP, play a pivotal role in the bioavailable pool of marine P (Martin et al. 2014, Diaz et al. 2018, 2019, Li et al. 2019, Sanz-Luque et al. 2020). PolyP emerges as a crucial nutritional P source, particularly under Pi deficiency, supporting the growth of eukaryotic phytoplankton (Diaz et al. 2018, 2019), heterotrophic bacteria (Adams et al. 2022), and *Synechococcus* WH8102 (Moore et al. 2005). This study further elucidates the importance of PolyP in open-ocean and coastal strains of *Synechococcus* and characterizes the potential for AP to drive its bioavailability and utilization. Our findings echo previous observations of the preferential degradation of P-anhydrides over P-esters, a phenomenon observed in diatoms of the genus *Thalassiosira* (Diaz et al. 2018, 2019), thus suggesting that P-anhydrides may substantially contribute to the nutritional DOP demand of phytoplankton. The relatively low concentration of P-anhydride containing compounds in natural marine DOP standing stocks could be explained by rapid microbial cycling (Young and Ingall 2010, Martin et al. 2014, Diaz et al. 2016, Bell et al. 2017, 2020). While AP activity has traditionally been a measure of P-ester hydrolysis, our study underscores its substantial substrate flexibility, including for short-chain P-anhydride hydrolysis. Notably, this flexibility varies between the *Synechococcus* WH8102 and WH5701 strains. A comprehensive understanding of DOP bioavailability necessitates the characterization of the enzymes involved. This study emphasizes the importance of further characterizing these enzymes, including AP flexibility for different DOP bond-classes and within taxonomic groups. These insights contribute to our understanding of marine nutrient cycling and have implications for ecosystem dynamics and biogeochemical processes.

## Acknowledgements

We thank Jamee Adams and Chau-Wen Chou for processing the proteomics samples and Jacob Schory Copple and Sofia Sánchez-Zárate for their contributions to the growth on DOP experiment. The mass spectrometry proteomics data have been deposited to the ProteomeXchange Consortium via the PRIDE partner repository with the dataset identifier PXD051991 and 10.6019/PXD051991.

## Author contributions

Emily M. Waggoner (Data curation, Formal analysis, Investigation, Methodology, Validation, Visualization, Writing – original draft, Writing – review & editing), Kahina Djaoudi (Formal analysis, Methodology, Validation, Visualization, Writing – review & editing), Julia M. Diaz (Conceptualization, Formal analysis, Funding acquisition, Methodology, Project administration, Validation, Writing – review & editing), and Solange Duhamel (Conceptualization, Data curation, Formal analysis, Funding acquisition, Investigation, Methodology, Project administration, Resources, Supervision, Validation, Writing – original draft, Writing – review & editing)

## Supplementary data

Supplementary data is available at *FEMSEC Journal* online.

*Conflict of interest*: None declared.

## Funding

This work was supported by the National Science Foundation (OCE-1737083, OCE-2001212, and OCE-2245249 to S.D., and OCE-1736967, OCE-1948042, OCE-1559124, OCE-2015310 and OCE-2245248 to J.M.D.), the Simons Foundation (678537 to J.M.D.) and in part by the National Institute of Health (T32 GM136536 to E.M.W.).

## References

Adams JC, Steffen R, Chou C *et al.* Dissolved organic phosphorus utilization by the marine bacterium *Ruegeria pomeroyi* DSS -3 reveals chain length-dependent polyphosphate degradation. *Environ Microbiol* 2022;**24**:2259–69.

Ammerman JW, Azam F. Bacterial 5-nucleotidase in aquatic ecosystems: a novel mechanism of phosphorus regeneration. *Science* 1985;**227**:1338–40.

Armstrong FAJ, Williams PM, Strickland JDH. Photo-oxidation of organic matter in sea water by ultra-violet radiation, analytical and other applications. *Nature* 1966;**211**:481–3.

Baltar F, De Corte D, Thomson B *et al.* Teasing apart the different size pools of extracellular enzymatic activity in the ocean. *Sci Total Environ* 2019;**660**:690–6.

Bell DW, Pellechia P, Chambers LR *et al.* Isolation and molecular characterization of dissolved organic phosphorus using electrodialysis-reverse osmosis and solution 31P-NMR. *Limnol Oceanogr Methods* 2017;**15**:436–52.

Bell DW, Pellechia PJ, Ingall ED *et al.* Resolving marine dissolved organic phosphorus (DOP) composition in a coastal estuary. *Limnol Oceanogr* 2020;**65**:2787–99.

Benitez-Nelson CR, Buesseler KO. Variability of inorganic and organic phosphorus turnover rates in the coastal ocean. *Nature* 1999;**398**:502–5.

Benitez-Nelson CR, O'Neill L, Kolowith LC *et al.* Phosphonates and particulate organic phosphorus cycling in an anoxic marine basin. *Limnol Oceanogr* 2004;**49**:1593–604.

Bertilsson S, Berglund O, Karl DM *et al.* Elemental composition of marine *Prochlorococcus* and *Synechococcus*: implications for the ecological stoichiometry of the sea. *Limnol Oceanogr* 2003;**48**:1721–31.

Björkman KM, Duhamel S, Church MJ *et al.* Spatial and temporal dynamics of inorganic phosphate and adenosine-5′-triphosphate in the North Pacific Ocean. *Front Mar Sci* 2018;**5**. https://doi.org/10.3389/fmars.2018.00235.

Bock N, Van Wambeke F, Dion M *et al.* Microbial community structure in the western tropical South Pacific. *Biogeosciences* 2018;**15**:3909–25.

Browning TJ, Moore CM. Global analysis of ocean phytoplankton nutrient limitation reveals high prevalence of co-limitation. *Nat Commun* 2023;**14**:5014.

Cembella AD, Antia NJ, Harrison PJ *et al.* The utilization of inorganic and organic phosphorous compounds as nutrients by eukaryotic microalgae: a multidisciplinary perspective: part 2. *CRC Crit Rev Microbiol* 1984;**11**:13–81.

Christie-Oleza JA, Armengaud J, Guerin P *et al.* Functional distinctness in the exoproteomes of marine *Synechococcus*. *Environ Microbiol* 2015;**17**:3781–94.

Cox A, Saito M. Proteomic responses of oceanic *Synechococcus* WH8102 to phosphate and zinc scarcity and cadmium additions. *Front Microbiol* 2013;**4**:387.

Diaz J, Ingall E, Benitez-Nelson C *et al.* Marine polyphosphate: a key player in geologic phosphorus sequestration. *Science* 2008;**320**:652–5.

Diaz JM, Björkman KM, Haley ST *et al.* Polyphosphate dynamics at Station ALOHA, North Pacific subtropical gyre. *Limnol Oceanogr* 2016;**61**:227–39.

Diaz JM, Holland A, Sanders JG *et al.* Dissolved organic phosphorus utilization by phytoplankton reveals preferential degradation of polyphosphates over phosphomonoesters. *Front Mar Sci* 2018;**5**:380.

Diaz JM, Steffen R, Sanders JG *et al.* Preferential utilization of inorganic polyphosphate over other bioavailable phosphorus sources by the model diatoms *Thalassiosira* spp. *Environ Microbiol* 2019;**21**:2415–25.

Djaoudi K, Van Wambeke F, Coppola L *et al.* Sensitive determination of the dissolved phosphate pool for an improved resolution of its vertical variability in the surface layer: new views in the P-depleted Mediterranean Sea. *Front Mar Sci* 2018;**5**:234.

Donald KM, Scanlan DJ, Carr NG *et al.* Comparative phosphorus nutrition of the marine cyanobacterium *Synechococcus* WH7803 and the marine diatom *Thalassiosira weissflogii*. *J Plankton Res* 1997;**19**:1793–813.

Duhamel S, Björkman K, Doggett J *et al.* Microbial response to enhanced phosphorus cycling in the North Pacific Subtropical Gyre. *Mar Ecol Prog Ser* 2014;**504**:43–58.

Duhamel S, Björkman KM, Wambeke FV *et al.* Characterization of alkaline phosphatase activity in the North and South Pacific subtropical gyres: implications for phosphorus cycling. *Limnol Oceanogr* 2011;**56**:1244–54.

Duhamel S, Diaz JM, Adams JC *et al.* Phosphorus as an integral component of global marine biogeochemistry. *Nat Geosci* 2021;**14**:359–68.

Duhamel S, Dyhrman ST, Karl DM. Alkaline phosphatase activity and regulation in the North Pacific Subtropical Gyre. *Limnol Oceanogr* 2010;**55**:1414–25.

Filella A, Riemann L, Van Wambeke F *et al.* Contrasting roles of DOP as a source of phosphorus and energy for marine diazotrophs. *Front Mar Sci* 2022;**9**:923765.

Fu F-X, Zhang Y, Feng Y *et al.* Phosphate and ATP uptake and growth kinetics in axenic cultures of the cyanobacterium *Synechococcus* CCMP 1334. *Eur J Phycol* 2006;**41**:15–28.

Granzow BN, Sosa OA, Gonnelli M *et al.* A sensitive fluorescent assay for measuring carbon-phosphorus lyase activity in aquatic systems. *Limnol Oceanogr Methods* 2021;**19**;235–44.

Hansen HP, Koroleff F. Determination of nutrients. In: *Methods of Seawater Analysis*. Hoboken: Wiley, 1999, 159–228.

Heldal M, Scanlan DJ, Norland S *et al.* Elemental composition of single cells of various strains of marine *Prochlorococcus* and *Synechococcus* using X-ray microanalysis. *Limnol Oceanogr* 2003;**48**:1732–43.

Holtz KM, Stec B, Kantrowitz ER. A model of the transition state in the alkaline phosphatase reaction. *J Biol Chem* 1999;**274**:8351–4.

Huang R, Wan B, Hultz M *et al.* Phosphatase-mediated hydrolysis of linear polyphosphates. *Environ Sci Technol* 2018;**52**:1183–90.

Hull DK, Ruttenberg KC. Dissolved organic phosphorus molecular weight fractionation and apparent bioavailability quantified via coupled sequential ultrafiltration and enzyme hydrolysis. *Limnol Oceanogr Methods* 2022;**20**:467–81.

Ilikchyan IN, Mckay RM, Kutovaya OA *et al.* Seasonal expression of the picocyanobacterial phosphonate transporter gene phnD in the Sargasso Sea. *Front Microbiol* 2010;**1**:135.

Ilikchyan IN, McKay RML, Zehr JP *et al.* Detection and expression of the phosphonate transporter gene phnD in marine and freshwater picocyanobacteria. *Environ Microbiol* 2009;**11**:1314–24.

Kamat SS, Raushel FM. The enzymatic conversion of phosphonates to phosphate by bacteria. *Curr Opin Chem Biol* 2013;**17**:589–96.

Kamennaya NA, Geraki K, Scanlan DJ *et al.* Accumulation of ambient phosphate into the periplasm of marine bacteria is proton motive force dependent. *Nat Commun* 2020;**11**:2642.

Karl DM, Björkman KM. Dynamics of dissolved organic phosphorus. In: *Biogeochemistry of Marine Dissolved Organic Matter*. Amsterdam: Elsevier, 2015, 233–334.

Karl DM, Tien G. MAGIC: a sensitive and precise method for measuring dissolved phosphorus in aquatic environments. *Limnol Oceanogr* 1992;**37**:105–16.

Kolowith LC, Ingall ED, Benner R. Composition and cycling of marine organic phosphorus. *Limnol Oceanogr* 2001;**46**:309–20.

Kretz CB, Bell DW, Lomas DA *et al.* Influence of growth rate on the physiological response of marine *Synechococcus* to phosphate limitation. *Front Microbiol* 2015;**6**:85.

Krom MD, Emeis K-C, Van Cappellen P. Why is the Eastern Mediterranean phosphorus limited?. *Prog Oceanogr* 2010;**85**:236–44.

Kutovaya OA, McKay RML, Bullerjahn GS. Detection and expression of genes for phosphorus metabolism in picocyanobacteria from the Laurentian Great Lakes. *J Gt Lakes Res* 2013;**39**:612–21.

Letscher RT, Wang WL, Liang Z *et al.* Regionally variable contribution of dissolved organic phosphorus to marine annual net community production. *Glob Biogeochem Cycles* 2022;**36**. https://doi.org/10.1029/2022GB007354.

Li J, Plouchart D, Zastepa A *et al.* Picoplankton accumulate and recycle polyphosphate to support high primary productivity in coastal Lake Ontario. *Sci Rep* 2019;**9**:19563.

Lin S, Litaker RW, Sunda WG. Phosphorus physiological ecology and molecular mechanisms in marine phytoplankton. *J Phycol* 2016;**52**:10–36.

Lin X, Guo C, Li L *et al.* Non-conventional metal ion cofactor requirement of dinoflagellate alkaline phosphatase and translational regulation by phosphorus limitation. *Microorganisms* 2019;**7**:232.

Lomas MW, Burke AL, Lomas DA *et al.* Sargasso Sea phosphorus biogeochemistry: an important role for dissolved organic phosphorus (DOP). *Biogeosciences* 2010;**7**;695–710.

Lopez JS, Garcia NS, Talmy D *et al.* Diel variability in the elemental composition of the marine cyanobacterium *Synechococcus*. *J Plankton Res* 2016;**38**:1052–61.

Lorenz B, Schröder HC. Mammalian intestinal alkaline phosphatase acts as highly active exopolyphosphatase. *Biochim Biophys Acta BBA Protein Struct Mol Enzymol* 2001;**1547**:254–61.

Martin P, Dyhrman ST, Lomas MW *et al.* Accumulation and enhanced cycling of polyphosphate by Sargasso Sea plankton in response to low phosphorus. *Proc Natl Acad Sci USA* 2014;**111**:8089–94.

Martin P, Lauro FM, Sarkar A *et al.* Particulate polyphosphate and alkaline phosphatase activity across a latitudinal transect in the tropical Indian Ocean. *Limnol Oceanogr* 2018;**63**:1395–406.
McCarren J, Heuser J, Roth R *et al.* Inactivation of swmA results in the loss of an outer cell layer in a swimming *Synechococcus* strain. *J Bacteriol* 2005;**187**:224–30.
McGrath JW, Ternan NG, Quinn JP. Utilization of organophosphonates by environmental micro-organisms. *Lett Appl Microbiol* 1997;**24**:69–73.
Moore CM, Mills MM, Arrigo KR *et al.* Processes and patterns of oceanic nutrient limitation. *Nat Geosci* 2013;**6**:701–10.
Moore L, Ostrowski M, Scanlan D *et al.* Ecotypic variation in phosphorus-acquisition mechanisms within marine picocyanobacteria. *Aquat Microb Ecol* 2005;**39**:257–69.
Nagarkar M, Wang M, Valencia B *et al.* Spatial and temporal variations in *Synechococcus* microdiversity in the Southern California coastal ecosystem. *Environ Microbiol* 2021;**23**:252–66.
Nausch M, Achterberg EP, Bach LT *et al.* Concentrations and uptake of dissolved organic phosphorus compounds in the Baltic Sea. *Front Mar Sci* 2018;**5**:386.
Nedoma J, Van Wambeke F, Štrojsová A *et al.* Affinity of extracellular phosphatases for ELF97 phosphate in aquatic environments. *Mar Freshw Res* 2007;**58**:454.
Palenik B, Brahamsha B, Larimer FW *et al.* The genome of a motile marine *Synechococcus*. *Nature* 2003;**424**:1037–42.
Palenik B, Ren Q, Dupont CL *et al.* Genome sequence of *Synechococcus* CC9311: insights into adaptation to a coastal environment. *Proc Natl Acad Sci USA* 2006;**103**:13555–9.
Parnell AE, Mordhorst S, Kemper F *et al.* Substrate recognition and mechanism revealed by ligand-bound polyphosphate kinase 2 structures. *Proc Natl Acad Sci USA* 2018;**115**:3350–5.
Quinn JP, Kulakova AN, Cooley NA *et al.* New ways to break an old bond: the bacterial carbon–phosphorus hydrolases and their role in biogeochemical phosphorus cycling. *Environ Microbiol* 2007;**9**:2392–400.
Ranjit P, Varkey D, Shah BS *et al.* Substrate specificity and ecological significance of PstS homologs in phosphorus uptake in marine *Synechococcus* sp. WH8102. *Microbiol Spectr* 2024;**12**:e02786–23.
Reid TW, Wilson IB. 17 *E. coli* alkaline phosphatase. In: Boyer PD (ed.), *The Enzymes*. Vol. **4**. Cambridge: Academic Press, 1971, 373–415.
Repeta DJ, Ferrón S, Sosa OA *et al.* Marine methane paradox explained by bacterial degradation of dissolved organic matter. *Nat Geosci* 2016;**9**:884–7.
Saad EM, Longo AF, Chambers LR *et al.* Understanding marine dissolved organic matter production: compositional insights from axenic cultures of *Thalassiosira pseudonana Limnol Oceanogr* 2016;**61**:2222–33.
Santos-Beneit F. The pho regulon: a huge regulatory network in bacteria. *Front Microbiol* 2015;**6**:402.
Sanz-Luque E, Bhaya D, Grossman AR. Polyphosphate: a multifunctional metabolite in cyanobacteria and algae. *Front Plant Sci* 2020;**11**:938.
Sato M, Sakuraba R, Hashihama F. Phosphate monoesterase and diesterase activities in the North and South Pacific Ocean. *Biogeosciences* 2013;**10**:7677–88.
Scanlan DJ, Ostrowski M, Mazard S *et al.* Ecological genomics of marine picocyanobacteria. *Microbiol Mol Biol Rev* 2009;**73**:249–99.
Shah BS, Ford BA, Varkey D *et al.* Marine picocyanobacterial PhnD1 shows specificity for various phosphorus sources but likely represents a constitutive inorganic phosphate transporter. *ISME J* 2023;**17**:1040–51.
Sisma-Ventura G, Rahav E. DOP stimulates heterotrophic bacterial production in the oligotrophic southeastern Mediterranean coastal waters. *Front Microbiol* 2019;**10**:1913.
Sohm JA, Ahlgren NA, Thomson ZJ *et al.* Co-occurring *Synechococcus* ecotypes occupy four major oceanic regimes defined by temperature, macronutrients and iron. *ISME J* 2016;**10**:333–45.
Sosa OA, Repeta DJ, DeLong EF *et al.* Phosphate-limited ocean regions select for bacterial populations enriched in the carbon–phosphorus lyase pathway for phosphonate degradation. *Environ Microbiol* 2019;**21**:2402–14.
Srivastava A, Saavedra DEM, Thomson B *et al.* Enzyme promiscuity in natural environments: alkaline phosphatase in the ocean. *ISME J* 2021;**15**:1–9.
Stosiek N, Talma M, Klimek-Ochab M. Carbon-phosphorus lyase—the state of the art. *Appl Biochem Biotechnol* 2020;**190**:1525–52.
Su Z, Olman V, Xu Y. Computational prediction of pho regulons in cyanobacteria. *BMC Genomics* 2007;**8**:156.
Tai V, Palenik B. Temporal variation of *Synechococcus* clades at a coastal Pacific Ocean monitoring site. *ISME J* 2009;**3**:903–15.
Tetu SG, Brahamsha B, Johnson DA *et al.* Microarray analysis of phosphate regulation in the marine cyanobacterium *Synechococcus* sp. WH8102. *ISME J* 2009;**3**:835–49.
Thomson B, Wenley J, Currie K *et al.* Resolving the paradox: continuous cell-free alkaline phosphatase activity despite high phosphate concentrations. *Mar Chem* 2019;**214**:103671.
Tiwari B, Singh S, Kaushik MS *et al.* Regulation of organophosphate metabolism in cyanobacteria. A review. *Microbiology* 2015;**84**:291–302.
Villarreal-Chiu J, Quinn J, McGrath J. The genes and enzymes of phosphonate metabolism by bacteria, and their distribution in the marine environment. *Front Microbiol* 2012;**3**:19.
Wang C, Lin X, Li L *et al.* Differential growth responses of marine phytoplankton to herbicide glyphosate. *PLoS One* 2016;**11**:e0151633.
Waterbury JB, Watson SW, Valois FW *et al.* Biological and ecological characterization of the marine unicellular cyanobacterium *Synechococcus*. *Can Bull Fish Aquat Sci* 1986;**214**:71–120.
Whisnant AR, Gilman SD. Studies of reversible inhibition, irreversible inhibition, and activation of alkaline phosphatase by capillary electrophoresis. *Anal Biochem* 2002;**307**:226–34.
Whitney LP, Lomas MW. Phosphonate utilization by eukaryotic phytoplankton. *Limnol Oceanogr Lett* 2019;**4**:18–24.
Yagil E, Beacham IR. Uptake of adenosine 5′-monophosphate by *Escherichia coli*. *J Bacteriol* 1975;**121**:401–5.
Yamaguchi H, Sakou H, Fukami K *et al.* Utilization of organic phosphorus and production of alkaline phosphatase by the marine phytoplankton, *Heterocapsa circularisquama, Fibrocapsa japonica* and *Chaetoceros ceratosporum*. *Plankton Biol Ecol* 2005;**52**; 67–75.
Young CL, Ingall ED. Marine dissolved organic phosphorus composition: insights from samples recovered using combined electrodialysis/reverse osmosis. *Aquat Geochem* 2010;**16**:563–74.
Yoza N, Onoue S, Kuwahara Y. Catalytic ability of alkaline phosphatase to promote P-O-P bond hydrolyses of inorganic diphosphate and triphosphate. *Chem Lett* 1997;**26**:491–2.
Yuan Z, Achterberg EP, Engel A *et al.* Switches between nitrogen limitation and nitrogen–phosphorus co-limitation in the subtropical North Atlantic Ocean. *Limnol Oceanogr* 2024;**9999**:1–9.
Zwirglmaier K, Jardillier L, Ostrowski M *et al.* Global phylogeography of marine *Synechococcus* and *Prochlorococcus* reveals a distinct partitioning of lineages among oceanic biomes. *Environ Microbiol* 2008;**10**:147–61.

**Received** 13 March 2024; **revised** 14 May 2024; **accepted** 12 July 2024